

Gas-Phase RNA and DNA Ions. 1. H/D Exchange of the $[M - H]^-$ Anions of Nucleoside 5'-Monophosphates (GMP, dGMP, AMP, dAMP, CMP, dCMP, UMP, dTMP), Ribose 5-Monophosphate, and 2-Deoxyribose 5-Monophosphate with D_2O and D_2S

Michael A. Freitas, Stone D.-H. Shi,[†] Christopher L. Hendrickson, and Alan G. Marshall*[‡]

Contribution from the National High Magnetic Field Laboratory, Florida State University, 1800 East Paul Dirac Drive, Tallahassee, Florida 32310

Received February 9, 1998

Abstract: H/D exchange from D_2O and D_2S to electrosprayed $[M - H]^-$ nucleoside 5'-monophosphate anions (GMP, dGMP, AMP, dAMP, CMP, dCMP, UMP, TMP) is examined by Fourier transform ion cyclotron resonance mass spectrometry at 9.4 T, along with sugar phosphate controls (ribose 5-monophosphate (R5P) and 2-deoxyribose 5-monophosphate (dR5P)). The relative exchange rates of the nucleotides with D_2O were $dR5P > dCMP > R5P > CMP > dAMP > UMP > AMP > dTMP \gg dGMP \gg GMP$, and with D_2S were $CMP > UMP \approx dTMP > dCMP > dAMP > AMP > R5P > dR5P \gg dGMP \gg GMP$. All exchange rates increase dramatically on changing from D_2O to D_2S , due to the smaller gas-phase acidity difference between exchange reagent and the nucleotide: $\Delta(\Delta H_{acid}) > 60 \text{ kcal mol}^{-1}$ for D_2O vs $\Delta(\Delta H_{acid}) > 20 \text{ kcal mol}^{-1}$ for D_2S . Ab initio calculations on model compounds at the MP2/6-31+G*/HF/6-31+G* level yield the following order of calculated acidities for each of the exchangeable hydrogens: $R_2O_3PO-H > R_2N-H > (R_2O-H \text{ on ribose}) > RN-H_2 > (R_2O-H \text{ on 2-deoxyribose})$. The present results provide a quantitative measure of proton exchange rates, in minutes for D_2S (rather than hours for D_2O) for gas-phase nucleotide anions, thereby opening up a wide range of extensions to chemically modified nucleotides as well as single-stranded and duplex RNAs and DNAs.

Introduction

Hydrogen/deuterium exchange is a powerful tool for examining the solution phase structure of proteins and peptides.^{1–15} Dating from the initial experiments performed by Lindström-Lang,¹ NMR and mass spectrometry have become the primary

tools to monitor the dynamics of H/D exchange of protein amide backbone protons. Although the overwhelming majority of H/D exchange studies focus on the solution phase, extension to the gas phase makes possible the analysis of H/D exchange without solvation effects. A recent review by Green and Lebrilla¹⁶ emphasizes the value of gas-phase ion–molecule reactions in the study of proteins and peptides.

Recently, Hoaglund et al. demonstrated the utility of ion mobility mass spectrometry for examining the shape of gas-phase oligonucleotide ions, $[T_{10} - nH]^{n-}$ and $[T_{10} + Na - nH]^{n-1}$.¹⁷ Gas-phase H/D exchange should prove equally useful for characterizing the gas-phase structure and dynamics of DNAs and RNAs. For example, Hemling et al. observed H/D exchange for the oligonucleotides $(dTp)_7dT$ and $(dTp)_{19}dT$ with ND_3 in the ionization region of their electrospray source.¹⁸ Recently, Robinson et al. investigated the H/D exchange kinetics of deoxynucleotide monophosphates with D_2O .¹⁹ They made the critical observation that 5'-monophosphate and 3'-monophosphate nucleotide anions undergo rapid H/D exchange, whereas 3'-5' cyclic monophosphate anions do not. The inescapable conclusion is that the conformationally flexible

[†] Member of the Department of Chemistry, Florida State University, Tallahassee, FL 32306.

(1) Englander, S. W.; Mayne, L.; Bal, Y.; Sosnick, T. R. *Protein Sci.* **1997**, *6*, 1101–1109.

(2) Englander, S. W.; Kallenbach, N. R. *Q. Rev. Biophys.* **1984**, *16*, 521–655.

(3) Englander, J. J.; Rogero, J. R.; Englander, S. W. *Anal. Biochem.* **1985**, *147*, 234–244.

(4) Englander, S. W.; Englander, J. J.; McKinnie, R. E.; Ackers, G. K.; Turner, G. J.; Westrick, J. A.; Gill, S. J. *Science* **1992**, *256*, 1684–1687.

(5) Englander, S. W.; Sosnick, T. R.; Englander, J. J.; Mayne, L. *Curr. Opin. Struct. Biol.* **1996**, *6*, 18–23.

(6) Zhang, Z.; Smith, D. L. *Protein Sci.* **1993**, *2*, 522–531.

(7) Winger, B. E.; Light-Wahl, K. J.; Rockwood, A. L.; Smith, R. D. *J. Am. Chem. Soc.* **1992**, *114*, 5897–5898.

(8) Wagner, D. S.; Anderegg, R. *J. Anal. Chem.* **1994**, *66*, 706–711.

(9) Smith, D. L.; Deng, Y.; Zhang, Z. *J. Mass Spectrom.* **1997**, *32*, 135–146.

(10) Smith, D. L.; Zhang, Z. *Mass Spectrom. Rev.* **1994**, *13*, 411–429.

(11) Knox, D. G.; Rosenberg, M. *Biopolymers* **1980**, *19*, 1049–1068.

(12) Gregory, R. B.; Rosenberg, A. In *Methods in Enzymology*; Hirs, C. H. W., Timasheff, S. N., Eds.; Academic Press: Orlando, FL, 1986; Vol. 131, pp 448–508.

(13) Cheng, X.; Fenselau, C. *Int. J. Mass Spectrom. Ion Processes* **1992**, *122*, 109–119.

(14) Katta, V.; Chait, B. T. *J. Am. Chem. Soc.* **1993**, *115*, 6317–6321.

(15) Woodward, C.; Simon, I.; Tuchsien, E. *Mol. Cell. Biochem.* **1982**, *48*, 135–160.

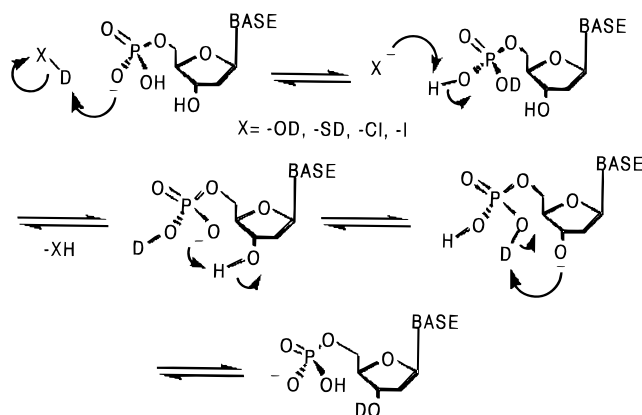
(16) Green, M. K.; Lebrilla, C. B. *Mass Spectrom. Rev.* **1997**, *16*, 53–71.

(17) Hoaglund, C. S.; Liu, Y.; Ellington, A. D.; Pagel, M.; Clemmer, D. E. *J. Am. Chem. Soc.* **1997**, *119*, 9051–9052.

(18) Hemling, M. E.; Conboy, J. J.; Bean, M. F.; Mentzer, M.; Carr, S. A. *J. Am. Soc. Mass Spectrom.* **1994**, *5*, 434–442.

(19) Robinson, J. M.; Greig, M. J.; Griffey, R. H.; Mohan, V.; Laude, D. A. *Anal. Chem.* **1998**, *70*, 3566–3571.

Scheme 1



phosphate group must therefore be the initial site for H/D exchange in gas-phase nucleotide anions. They proposed the mechanism shown in Scheme 1, in which the phosphate group undergoes rapid exchange followed by slow intramolecular exchange with other sites within the nucleotide.

In a broadly applicable generalization, DePuy and Bierbaum proposed that proton exchange between an anion and a neutral can be observed only if the neutral reagent is ~ 20 kcal mol $^{-1}$ less acidic than the anion.²⁰ Ausloos and Lias also showed that, for protonated compounds, proton exchange is not observed if the gas-phase basicity of the neutral base is greater than 20 kcal mol $^{-1}$ of the deuterated reagent.²¹ However, for amino acids and small peptide cations, proton exchange has been observed when the basicity difference is > 20 kcal mol $^{-1}$,^{22,23} presumably due to complexation of the exchange reagent with functional groups on the amino acids and peptides. Furthermore, for the exchange of chlorinated benzene anions with D₂O and ND₃, Chan and Enke found that the reaction efficiency decreased as the gas-phase acidity difference between the anion and neutral increased.²⁴ That behavior can be understood by examining the mechanism responsible for gas-phase exchange. At least two proton transfers must take place for H/D exchange to occur.²⁵ Experimental values for the acidity of nucleotides²⁶ and the two exchange reagents H₂O and H₂S²⁷ are listed in Table 1. If we take the acidity values of H₂O and D₂O as equal (also those of H₂S and D₂S), then the acidity difference between the respective exchange reagents and nucleotides is > 60 kcal mol $^{-1}$ for D₂O but only > 20 kcal mol $^{-1}$ for D₂S. However, assuming a 20 kcal mol $^{-1}$ energy benefit from the formation of an ion-molecule complex,²⁸ we estimate a barrier of > 40 kcal mol $^{-1}$ for the reaction of a deprotonated nucleotide with D₂O vs a thermoneutral reaction with D₂S (Scheme 2).

Here, our immediate goal is to demonstrate the effect of gas-phase acidity on the relative exchange rate of D₂O and D₂S with ribose 5-monophosphate (R5P), 2-deoxyribose 5-monophosphate (dR5P), and the biologically important mononucle-

(20) DePuy, D. H.; Bierbaum, V. M. *Acc. Chem. Res.* **1981**, *14*, 146–153.

(21) Ausloos, P.; Lias, S. G. *J. Am. Chem. Soc.* **1981**, *103*, 3641–3647.

(22) Gard, E.; Willard, D.; Bregar, J.; Green, M. K.; Lebrilla, C. *Org. Mass Spectrom.* **1993**, *28*, 1632–1639.

(23) Gard, E.; Green, M. K.; Bregar, J.; Lebrilla, C. *J. Am. Soc. Mass Spectrom.* **1994**, *5*, 623–631.

(24) Chan, S.; Enke, C. G. *J. Am. Soc. Mass Spectrom.* **1994**, *5*, 282–291.

(25) Squires, R. R.; Bierbaum, V. M.; Grabowski, J. J.; DePuy, C. H. *J. Am. Chem. Soc.* **1983**, *105*, 5187–5192.

(26) Green-Church, K. B.; Limbach, P. A., unpublished results.

(27) Lias, S. G.; Bartmess, J. E.; Liebman, J. F.; Holmes, J. L.; Levin, R. D.; Mallard, W. G. *J. Phys. Chem. Ref. Data* **1988**, *17* (Suppl. 1.)

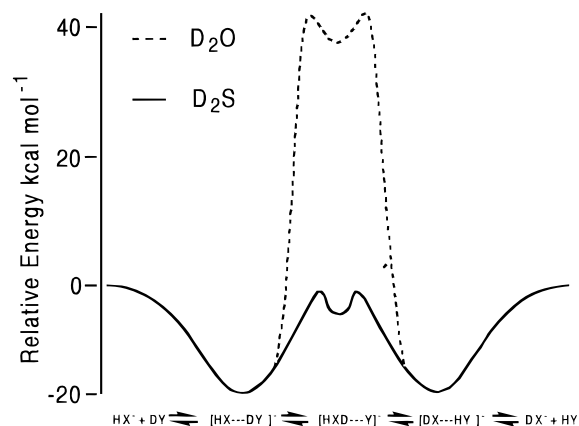
(28) Kebarle, P. *Annu. Rev. Phys. Chem.* **1977**, *28*, 445–476.

Table 1. Gas-Phase Acidities^a

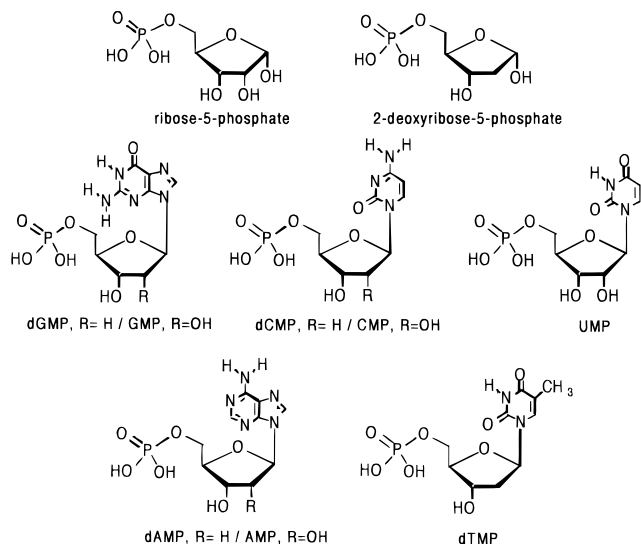
species/ exchange site	gas-phase acidity			
	expt	AM1 ^b	PM3 ^b	MP2 ^c
H ₂ O ^d	390.8			381.8
H ₂ S ^d	351.3 (±0.5)			346.0
dCMP ^e	328.5 (±5)			
CMP ^e	327.8 (±5)			
dAMP ^e	326.9 (±5)			
UMP ^e	327.0 (±5)			
AMP ^e	326.5 (±5)			
TMP ^e	327.1 (±5)			
dGMP ^e	330.3 (±5)			
GMP ^e	327.8 (±5)			
cytosine				
H-1		338.9	328.2	337.0
H-2		345.6	338.1	342.2
H-3		351.5	345.1	349.0
adenine				
H-1		332.9	327.9	326.6
H-2		349.0	340.0	347.6
H-3		350.0	340.9	348.9
uracil				
H-1				326.3
H-2				339.6
thymine				
H-1		328.0	322.3	327.1
H-2		344.1	336.7	339.4
guanine				
H-1		330.5	327.0	326.7
H-2		333.4	326.7	333.3
H-3		335.8	325.9	330.5
H-4		337.3	333.1	339.6
3-hydroxyfuran				361.2
syn-3,4-dihydroxyfuran				345.6
methylamine ^d	403.2 (±1.2)			400.4
aniline ^d	366.4 (±2.6)			364.1
imidazole ^d	350.2 (±2.6)	346.2	340.4	351.4
indole ^d	349.2 (±2.6)			341.6
formamide ^d	360.4 (±2.6)	366.3	356.4	356.1
dimethyl ^d	331.6 (±4.1)	340.0	342.0	320.7
phosphate ^d				

^a All values for gas-phase acidity reported in kcal mol $^{-1}$. ^b Reference 42. ^c Calculated at the MP2/6-31+G*/HF/6-31+G* level of theory. ^d Reference 27. ^e Measured by ion-molecule reaction equilibria.²⁶

Scheme 2



otides, guanosine 5'-monophosphate (GMP), 2'-deoxyguanosine 5'-monophosphate (dGMP), adenosine 5'-monophosphate (AMP), 2'-deoxyadenosine 5'-monophosphate (dAMP), cytidine 5'-monophosphate (CMP), 2'-deoxycytidine 5'-monophosphate (dCMP), thymidine 5'-monophosphate (dTMP), and uridine 5'-monophosphate (UMP). A larger goal is to speed up gas-phase H/D reactions so that they can be quantitated rapidly for a wide range of DNA and RNA mono- and polynucleotides.



Experimental Section

Experiments were performed by constant-infusion electrospray followed by external accumulation and ion injection into a home-built 9.4-T FT-ICR mass spectrometer described previously.^{29,30} Samples were infused into a 50- μm -i.d. fused silica needle at 300 nL min^{-1} at a concentration of 10 μM . Typical ESI conditions were as follows: needle voltage -3 kV; heated capillary current 3 A. Ions were accumulated in a linear octopole ion trap for 1–5 s and then transmitted to a three-section open cylindrical 4-in.-diameter Penning trap (trapping voltage -2V) through a second octopole ion guide. The most abundant monoisotopic $[\text{M} - \text{H}]^-$ ions were isolated by a combination of frequency sweep^{31,32} and stored-waveform inverse Fourier transform (SWIFT) excitation events.^{33,34} Upon isolation, parent ions were allowed to react with either D_2O or D_2S gas leaked into the vacuum system through a leak valve to achieve a neutral reagent partial pressure of 5×10^{-8} Torr measured by a Granville Phillips (Boulder, CO) model 274 ion gauge. The temperature of the neutral reagent inside the vacuum chamber was taken to be room temperature. Immediately following hydrogen/deuterium exchange, the ions were subjected to frequency sweep excitation (200 kHz to 1 MHz at 300 Hz/ μs) and direct-mode broad-band detection (128K word data points and 800-kHz bandwidth) Typical base pressure for the instrument varied from 0.5×10^{-9} to 1×10^{-9} Torr. Experiments were controlled by either an Odyssey data station (Finnigan Corp., Madison, WI) or a modular ICR data acquisition system (MIDAS)³⁵ controlled by use of Dynamic Data Exchange scripts. $[\text{M} - \text{H}]^-$ ions were allowed to react with the neutral reagent for 0–360 s, and the results was monitored at each of a minimum of six time intervals. Each reported ion relative abundance (calculated from three-point parabolic

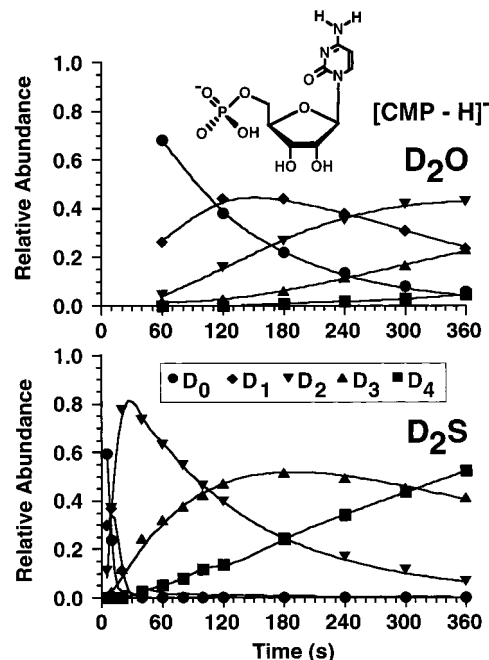


Figure 1. Reaction progress curves for cytosine 5'-monophosphate reacting with (top) D_2O at 5×10^{-8} Torr and (bottom) D_2S at 5×10^{-8} Torr.

interpolated peak heights) represents an average of four-repeated measurements. The ions may acquire excess internal energy during ionization, transfer, and isolation. However, the ions are rapidly cooled (<10 s) by collisions with the neutral exchange reagent as evidenced by the initial slope of the reaction progress curves.

Rate Constants. Rate constants were determined by fitting the experimental data with the KinFit program provided by Nicoll and Dearden.³⁶ A system of $N + 1$ (in which N is the number of observed exchanged hydrogens) differential equations models the exchange kinetics. A back-exchange term in which the reverse rate constant was assumed to be the same as the forward rate constant multiplied by the H content (in percent, 3% for D_2S and 0.1% for D_2O) of the neutral reagent was also included.^{22,23} For cases with a poor curve fit, the percent H content was also optimized. Data points with a relative abundance of <0.01 near the end of the exchange period were omitted from the rate constant extrapolation. An experimental reproducibility of $\pm 5\%$ for k_1 and k_2 and $\pm 70\%$ for k_3 was determined by repeating the reaction for dAMP + D_2S on three separate days. Figures 1 and 2 show typical reaction progress curves along with the fitted results for the reactions of D_2O and D_2S with CMP and GMP.

For the present systems, *site-specific* rate constants are difficult to assign for two reasons. First, even if all of the potentially exchangeable hydrogens are experimentally observed, we cannot be sure as to which is which unless one or more groups of hydrogens are chemically equivalent: e.g., one site with two chemically equivalent exchangeable hydrogens vs a different site with one exchangeable hydrogen. Second, it is often the case (as in this work) that not all of the hydrogens exchange, so that one cannot be sure which sites are exchangeable at all, let alone which are fast or slow. At this stage, we therefore simply report *relative* exchange rate constant magni-

(29) Senko, M. W.; Hendrickson, C. L.; Emmett, M. R.; Shi, S. D.-H.; Marshall, A. G. *J. Am. Soc. Mass Spectrom.* **1997**, *8*, 970–976.

(30) Senko, M. W.; Hendrickson, C. L.; Pasa-Tolic, L.; Marto, J. A.; White, F. M.; Guan, S.; Marshall, A. G. *Rapid Commun. Mass Spectrom.* **1996**, *10*, 1824–1828.

(31) Comisarow, M. B.; Marshall, A. G. *Chem. Phys. Lett.* **1974**, *26*, 489–490.

(32) Marshall, A. G.; Roe, D. C. *J. Chem. Phys.* **1980**, *73*, 1581–1590.

(33) Marshall, A. G.; Wang, T.-C. L.; Ricca, T. L. *J. Am. Chem. Soc.* **1985**, *107*, 7893–7897.

(34) Marshall, A. G.; Wang, T.-C. L.; Chen, L.; Ricca, T. L. *ACS* **1987**, *359*, 21–33.

(35) Senko, M. W.; Canterbury, J. D.; Guan, S.; Marshall, A. G. *Rapid Commun. Mass Spectrom.* **1996**, *10*, 1839–1844.

(36) Nicoll, J. B.; Dearden, D. V. *KinFit*; 1.0 ed.; Department of Chemistry and Biochemistry, Brigham Young University: Provo, UT, 1997.

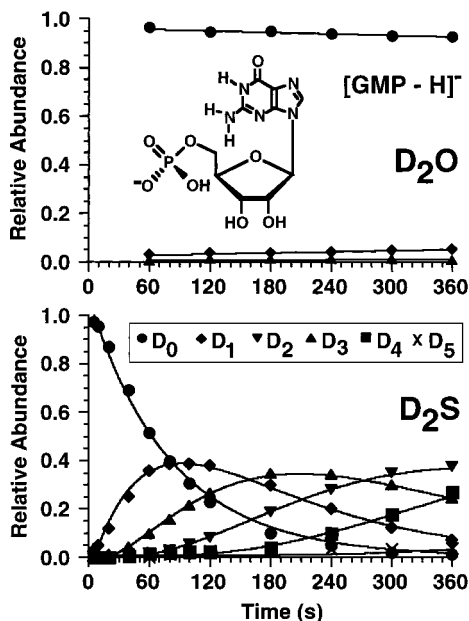


Figure 2. Reaction progress curves for guanosine 5'-monophosphate reacting with (top) D_2O at 5×10^{-8} Torr and (bottom) D_2S at 5×10^{-8} Torr.

tudes, to rank the exchange rate constants and reveal overall trends.¹⁶ Future experiments based on comparison of various substituted nucleotides will be needed for unequivocal assignments of rate constants to particular sites on the molecule.

Sample Preparation. The 5'-monophosphate nucleotides, D_2O (99.9% D), ribose 5-monophosphate, and 2-deoxyribose 5-monophosphate were purchased from the Sigma Chemical Co. (St. Louis, MO) and used without further purification. D_2S (97% D) was purchased from the Isotec Chemical Co. (Miamisburg, OH). The nucleotides and sugar phosphates were dissolved in 50:50 isopropyl alcohol/water and diluted to a final concentration of $10 \mu M$.

Computational Chemistry. Semiempirical and ab initio calculations were performed with PC GAMESS 4.1,³⁷ Gaussian 94W,³⁸ and Hyperchem 5.0 with the ChemPlus package (Hypercube Inc., Gainesville, FL). Molecular geometries were initially optimized at the AM1 level of theory.³⁹ Conformational analysis was conducted by the Usage Directed method available in the ChemPlus package (Hypercube Inc.) The lowest energy conformations were then optimized at the Restricted Hartree-Fock level of theory with the 6-31+G* basis set. The HF/6-

(37) Schmidt, M. W.; Baldridge, K. K.; Boatz, J. A.; Elbert, S. T.; Gordon, M. S.; Jensen, J. H.; Koseki, S.; Matsunaga, N.; Nguyen, K. A.; Su, S. J.; Windus, T. L.; Dupuis, M.; Montgomery, J. A. *J. Comput. Chem.* **1993**, *14*, 1347-1363.

(38) Frisch, M. J.; Trucks, G. W.; Schlegel, H. B.; Gill, P. M. W.; Johnson, B. G.; Robb, M. A.; Cheeseman, J. R.; Keith, T.; Petersson, G. A.; Montgomery, J. A.; Raghavachari, K.; Al-Laham, M. A.; Zakrzewski, V. G.; Ortiz, J. V.; Foresman, J. B.; Cioslowski, J.; Stefanov, B. B.; Nanayakkara, A.; Challacombe, M.; Peng, C. Y.; Ayala, P. Y.; Chen, W.; Wong, M. W.; Andres, J. L.; Replogle, E. S.; Gomperts, R.; Martin, R. L.; Fox, D. J.; Binkley, J. S.; Defrees, D. J.; Baker, J.; Stewart, J. P.; Head-Gordon, M.; Gonzalez, C.; Pople, J. A. *Gaussian 94*, Revision E.3 ed.; Frisch, M. J.; Trucks, G. W.; Schlegel, H. B.; Gill, P. M. W.; Johnson, B. G.; Robb, M. A.; Cheeseman, J. R.; Keith, T.; Petersson, G. A.; Montgomery, J. A.; Raghavachari, K.; Al-Laham, M. A.; Zakrzewski, V. G.; Ortiz, J. V.; Foresman, J. B.; Cioslowski, J.; Stefanov, B. B.; Nanayakkara, A.; Challacombe, M.; Peng, C. Y.; Ayala, P. Y.; Chen, W.; Wong, M. W.; Andres, J. L.; Replogle, E. S.; Gomperts, R.; Martin, R. L.; Fox, D. J.; Binkley, J. S.; Defrees, D. J.; Baker, J.; Stewart, J. P.; Head-Gordon, M.; Gonzalez, C.; Pople, J. A.; Gaussian, Inc.: Pittsburgh, PA, 1995.

(39) Dewar, M. J. S.; Zoebisch, E. G.; Healy, E. F.; Stewart, J. P. *J. Am. Chem. Soc.* **1985**, *107*, 3902.

31+G*-optimized geometries were used to calculate HF/6-31+G* vibrational frequencies to obtain zero-point energy corrections. Zero-point energies were scaled (downward) by a factor of 0.9.⁴⁰ The MP2/6-31+G* single-point energies were then calculated to correct for electron correlation.

Results and Discussion

Gas-Phase Acidities of Nucleotides and Nucleobases. The compounds listed in Table 1 were chosen as models for estimating the gas-phase acidity of the different exchange sites within the nucleotides. Although attempts have been made to determine the relative order of acidity between nucleobases, those methods did not address the experimental acidity of different individual exchange sites within the nucleobase.^{41,42} To determine the acidities of each exchange site, we therefore resort to ab initio molecular orbital theory. Equations 1a and 1b illustrate how gas-phase acidity (GA) is estimated from

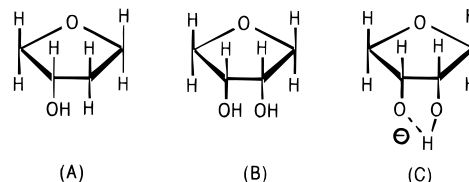


$$GA = E_c^0(A^-) - E_c^0[HA] + \Delta ZPE \quad (1b)$$

electronic and vibrational energies from electronic structure calculations, in which E_c^0 denotes electronic energy and ZPE denotes the zero-point energy reduced by a scale factor of 0.9.⁴⁰ The basis set should include diffuse functions for calculation of the geometry and energies of anions.⁴³ For that reason, we chose the 6-31+G* basis set as a compromise between accuracy and expense. The adequacy of that level of theory has been examined by comparing theoretical and experimental acidities²⁷ for model compounds containing functional groups found in nucleobases. The calculated and experimental values were in reasonable agreement for all model systems.

The acidity of the phosphate group was modeled by dimethyl phosphate. Our ab initio calculations suggest that the phosphate group is the most acidic site within the nucleotide (i.e., exhibits the smallest gas-phase acidity), as expected. Our calculated acidity of dimethyl phosphate also agrees well with the experimental values for the gas-phase acidities of nucleotides.²⁶

To model the gas-phase acidity of the hydroxyl groups on the ribose and deoxyribose sugar units of the nucleotide, we chose 3-hydroxyfuran (**A**) and *syn*-3,4-dihydroxyfuran (**B**). Our



ab initio calculations indicate that the neighboring *syn* hydroxyl group on the *syn*-3,4-dihydroxyfuran can stabilize the anion **C** produced upon deprotonation. The anomalously high calculated acidity for 3-hydroxyfuran may be due to conformational changes upon deprotonation. In addition, lower energy conformations may not have been revealed during conformational analysis.

(40) Scott, A. P.; Radom, L. *J. Phys. Chem.* **1996**, *100*, 16502-16513.

(41) Habibi-Goudarzi, S.; McLuckey, S. A. *J. Am. Soc. Mass Spectrom.* **1995**, *6*, 102-113.

(42) Rodgers, M. T.; Campbell, S.; Marzluff, E. M.; Beauchamp, J. L. *Int. J. Mass Spectrom. Ion Processes* **1994**, *137*, 121-149.

(43) Foresman, J. B.; Frisch, G. *Exploring Chemistry with Electronic Structure Methods*; 2nd ed.; Gaussian, Inc.: Pittsburgh, PA, 1993.

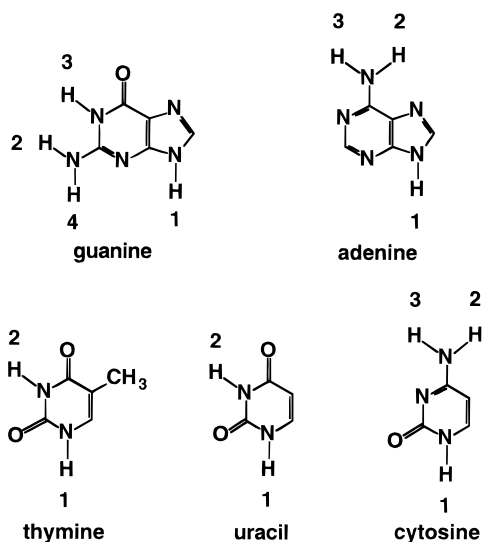


Figure 3. Nucleobase sites for which the gas-phase acidity was calculated. The acidity values in Table 1 correspond to these numbers.

Acidities for each of the potential exchange sites within the individual nucleobases were also calculated (see Figure 3). The number of exchangeable hydrogens (note that the hydrogen at the 1-position is not present when the base is attached to a sugar) for each nucleobase is as follows: guanine (3), adenine (2), cytosine (2), thymine (1), and uracil (1). The corresponding nucleotide monophosphates will have an additional two or three exchangeable hydrogens for deoxyribose and ribose sugars, respectively. Those acidity values were compared with those calculated by Rodgers et al. at the AM1 and PM3 semiempirical levels of theory.⁴² Both the semiempirical and ab initio results predict the same ordering of acidities for the sites within the nucleobases: cytosine, adenine, and thymine. However, for guanine, each level of theory predicts a different ordering. Unfortunately, the only experimental gas-phase acidity data available for the nucleobases are for the site for which we do not observe H/D exchange.^{41,42} In summary, our ab initio results predict that the most favored sites of exchange, based on the gas-phase acidities of each site, should follow the order, RO₃-PO-H > R₂N-H > (R₂O-H on ribose) > RN-H₂ > (R₂O-H on 2'-deoxyribose). These data clearly demonstrate that the phosphate site is the most acidic site within the molecule and therefore most likely to undergo initial exchange. Furthermore, the calculations show that the hydrogens on the hydroxyl groups can compete with the amine hydrogens for exchange. However, without the ability to assess the site-specific rate constants, it is difficult to identify exchange sites from the relative apparent exchange rate constants and the ab initio calculations.

Reactions of Nucleotides with D₂O. The apparent relative exchange rate constants for the [M - H]⁻ nucleotide anions reacting with D₂O at an apparent pressure of 5 × 10⁻⁸ Torr are given in Table 2. The relative rate for the first exchange follows the order, dR5P > dCMP > R5P > CMP > dAMP > UMP > AMP > dTMP ≫ dGMP ≫ GMP. Our results for the deoxynucleotides agree well with the experimental results of Robinson et al., for which exchange with D₂O was measured at a pressure of 1 × 10⁻⁷ Torr.¹⁹

In none of the reactions does complete exchange occur before 360 s. Only dR5P (three exchangeable hydrogens) and R5P (four exchangeable hydrogens) approach complete exchange (Figures 4a and 5a). In all cases, the deoxynucleotides exchange more rapidly than their ribose derivatives. The greatest rate

Table 2. Relative Apparent Rate Constants^a for the [M - H]⁻ Nucleotides Reacting with D₂O^b

species	k ₁	k ₂	k ₃	k ₄
dR5P	1.00	0.59	0.18	
dCMP	0.82	0.38	<0.02	
R5P	0.77	0.56	0.36	0.19
CMP	0.60	0.39	0.20	0.13
dAMP	0.49	0.27	<0.02	0.11
UMP	0.35	0.20	0.08	
AMP	0.32	0.16	<0.02	
TMP	0.23	0.15	0.06	
dGMP	0.03	0.07		
GMP	< 0.02	0.03		

^a All rate constants are reported relative to 2-deoxyribose 5-monophosphate + D₂O, and assigned an error of ± 0.02. ^b D₂O apparent pressure 5.0 × 10⁻⁸ Torr.

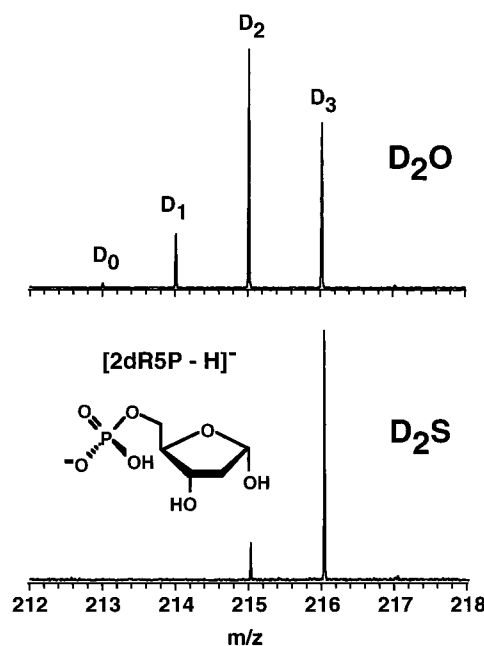
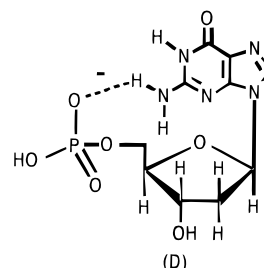


Figure 4. FT-ICR mass spectra for 2-deoxyribose-5-monophosphate after a reaction period of 360 s with (top) D₂O at 5 × 10⁻⁸ Torr and (bottom) D₂S at 5 × 10⁻⁸ Torr.

effect derives from base substitution. The addition of a nucleobase to the sugar-phosphate slows the exchange rate dramatically. Particularly slow exchange is observed for GMP and dGMP. It has previously been proposed that the [M - H]⁻ ion of dGMP may be stabilized by hydrogen bonding of the phosphate anion to the amino hydrogen on the nucleobase D.^{19,42,44} That effect of intramolecular complexation produces



a conformation that would result in a lower number of collisions with proper orientation for exchange.

(44) Phillips, D. R.; McCloskey, J. A. *Int. J. Mass Spectrom. Ion Processes* **1993**, *128*, 61–82.

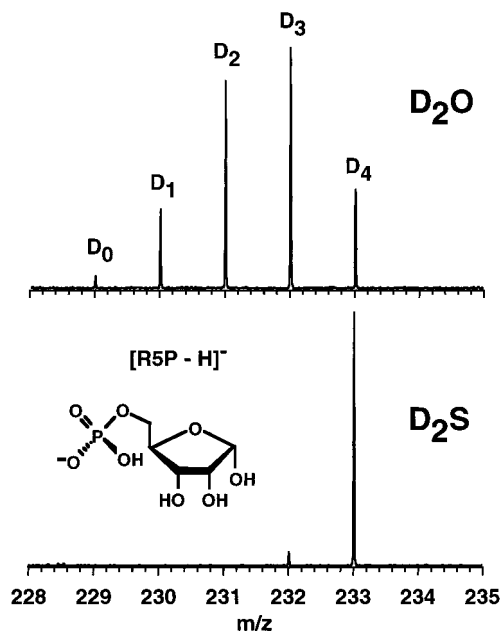


Figure 5. FT-ICR mass spectra for ribose 5-phosphate after a reaction period of 360 s with (top) D_2O at 5×10^{-8} Torr and (bottom) D_2S at 5×10^{-8} Torr.

Table 3. Relative Apparent Rate Constants^a for the $[M - H]^-$ Nucleotides Reacting with D_2S ^b

species	k_1	k_2	k_3	k_4	k_5
CMP	26.0	22.7	1.0	<0.5	
UMP	22.1	22.2	<0.5		
TMP	22.1	15.2	<0.5		
dCMP	18.6	16.8	0.6	< 0.5	
dAMP	17.9	15.4	<0.5		
AMP	16.2	16.4	<0.5		
R5P	14.2	20.7	4.5	3.7	
dR5P	13.0	21.9	10.4		
dGMP	11.5	7.3	3.9	<0.5	<0.5
GMP	1.5	1.3	0.9	<0.5	<0.5

^a All rate constants are reported relative to 2-deoxyribose 5-monophosphate + D_2O , scaled by appropriate ion gauge sensitivity factors,⁴⁵ and assigned an error of ± 0.5 . ^b D_2S apparent pressure 5.0×10^{-8} Torr.

Reactions of Nucleotides with D_2S . The apparent relative exchange rate constants for the nucleotide $[M - H]^-$ ions reacting with D_2S at an apparent pressure of 5.0×10^{-8} Torr are given in Table 3. Those data are reported relative to the rate constant for $D_2O + dR5P$ and scaled to correct for differences in ion gauge sensitivity for H_2O and H_2S (0.97 and 1.82).⁴⁵ The exchange rate constant order is as follows: $CMP > UMP = dTMP > dCMP > dAMP > AMP > R5P > dR5P \gg dGMP \gg GMP$. In every case, the exchange rate constant increases dramatically on going from D_2O to D_2S as the exchange reagent. In addition, the relative ordering of the rates for the nucleotides has changed. The reason for this change is unclear but may indicate that D_2S exchanges with the nucleotide anions via a mechanism different from D_2O . The most dramatic increase was for GMP and dGMP, which reacted slowest with both D_2O and D_2S . Figure 6 demonstrates the dramatic increase in exchange rate for D_2S relative to D_2O as the exchange reagent for GMP. In addition, the number of observable exchanges increases for dCMP, dGMP and GMP.

For almost all of the nucleotides, k_2 and k_1 are similar in magnitude, whereas $k_2 > k_1$ for ribose and deoxyribose

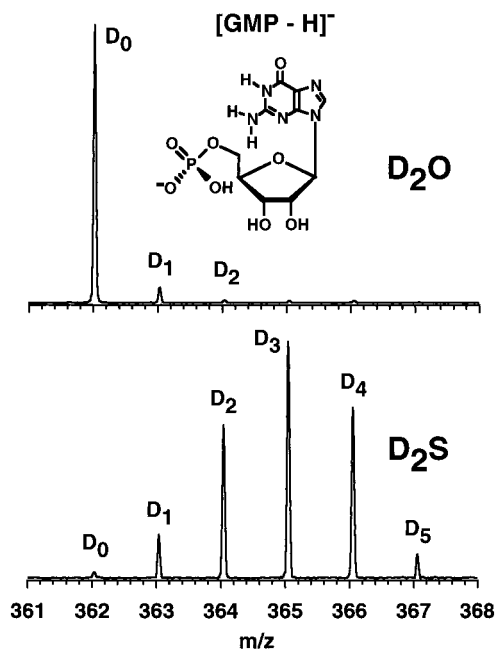


Figure 6. FT-ICR mass spectra for guanosine 5'-monophosphate after a reaction period of 360 s with (top) D_2O at 5×10^{-8} Torr and (bottom) D_2S at 5×10^{-8} Torr.

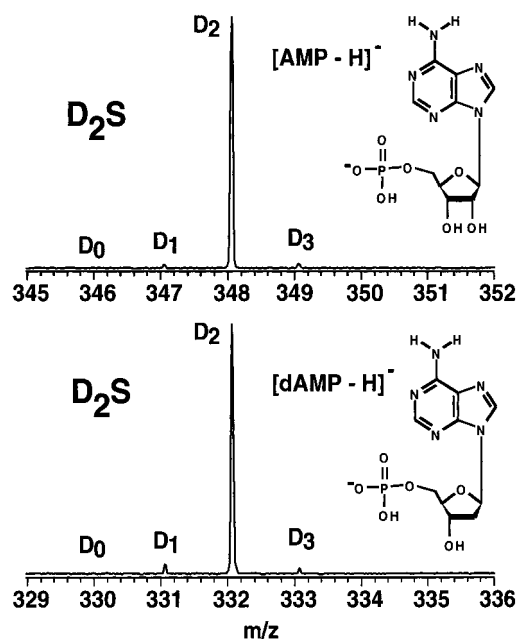


Figure 7. FT-ICR mass spectra for (top) adenosine 5'-monophosphate with D_2O at 5×10^{-8} Torr after a reaction period of 360 s and (bottom) 2'-deoxyadenosine 5'-monophosphate with D_2O at 5×10^{-8} Torr after a reaction period of 360 s.

monophosphate. Both R5P and dR5P undergo complete exchange after the 360-s time interval (Figures 4b and 5b). Thus, if the mechanism proposed by Robinson et al. is correct, the hydroxyl groups are readily accessible to the deuterated phosphate anion.¹⁹ That idea is further supported by the exchange behavior of dAMP, in which only two hydrogens exchange (Figure 7a). On the basis of the calculated sites for exchange, the amino hydrogens are equally favored thermodynamically as the hydroxyl hydrogen. However, AMP, which contains an additional hydroxyl group, only exchanged two hydrogens (Figure 7b). That unusual behavior for AMP, together with the large relative value of k_2 suggests the presence

(45) Bartmess, J. E.; Georgiadis, R. M. *Vacuum* **1983**, *33*, 149–153.

of more than one exchange mechanism. Further studies on the significance of the mobile phosphate anion as well as determination of which sites are exchanged in dAMP and AMP is warranted.

Gas Phase vs Solution. The H/D exchange of nucleotides is very different in the gas phase relative to solution phase. Gas-phase exchange of nucleotides is believed to proceed by a complex reaction mechanism involving intermolecular and intramolecular proton transfers. As in the cases of AMP and dAMP, sites with conformationally inaccessible hydrogens exchange slowly. However in the high pressure of an ESI source, oligonucleotides have been shown to undergo nearly complete exchange,¹⁸ in stark contrast to the exchange behavior seen here, suggesting that exchange in the ESI source is occurring in solution. Phillips and McCloskey examined solution-phase exchange by performing collision-induced dissociation on dinucleotides dissolved in deuterated glycerol.⁴⁴ Their fragment ions clearly indicate that all sites are readily exchanged in solution.

Conclusions and Directions for Future Work

Our ultimate goal is to perform (and explain) gas-phase H/D exchange for single- and double-stranded DNAs and RNAs, as a sensitive probe of the three-dimensional gas-phase structure(s) of DNAs and RNAs. To that end, the present results for mononucleotides and sugar phosphates provide a fundamental starting point for elucidating the mechanism of H/D exchange for larger systems. Specifically, the presently demonstrated dramatic increase in H/D exchange rate with D₂S relative to

D₂O shortens (from hours to minutes) the time required to measure such rates experimentally. The results are also more accurate (because fewer ions are lost from the ion trap during the measurement) and extend to less acidic analyte hydrogens (because slower H/D exchange rates become experimentally accessible). The extension to even more acidic DCl, DBr, and DI as potential negative-ion exchange reagents is being investigated. Extensions to di- and triphosphate nucleotides should reveal the effect of multiple negative charges on gas-phase nucleotide conformation (as revealed by H/D exchange rate). The anomalous behavior of AMP will be explored from the H/D exchange behavior of various derivatives of AMP and dAMP. Moreover, nucleotides with the phosphate group substituted with a carboxylic acid should clarify the role of an aprotic highly acidic group on the rate of H/D exchange. Finally, obvious extensions to single-stranded and duplex RNAs and DNAs should now be possible.

Acknowledgment. We thank J. M. Robinson and P. A. Limbach for sharing with us their unpublished results, D. V. Dearden and J. B. Nicoll for giving us their KinFit program, and C. B. Lebrilla and M. K. Green for providing their Mathematica notebooks for calculation of rate constants. This work was supported by the NSF National High Field FT-ICR Mass Spectrometry Facility (Grant CHE-94-13008), Florida State University, and the National High Magnetic Field Laboratory at Tallahassee, FL.

JA980449G